Load Torque and Moment of Inertia Identification for Permanent Magnet Synchronous Motor Drives Based on Sliding Mode Observer

Chuanqiang Lian, Fei Xiao, Shan Gao, and Jilong Liu

提出了一种基于滑模观测器的负载转矩识别方法，该方法考虑了惯性矩、电磁转矩和粘滞摩擦的不匹配。分析表明，选择合适的观测器参数可以很好地减弱振颤现象。

基于惯性矩失配会引起负载转矩观测误差的特性，提出了两种惯性矩识别方法，即直接计算法和比例积分调节器法。还对直流稳压器和PI稳压器的辨识误差进行了理论分析。

***Abstract*—In this paper, a load torque observer and two moment of inertia identification methods are developed for permanent magnet synchronous motor drive systems. First, the load torque identification method is proposed based on sliding mode observer, in which the mismatches of moment of inertia, electromagnetic torque, and viscous friction are all considered. It is analyzed that the chattering phenomenon will be well weakened if appropriate observer parameters are chosen. Second, based on the property that the mismatch of the moment of inertia will cause the load torque observation error, two types of moment of inertia identification methods, called direct calculation (DC) method and proportional integral (PI) regulator method, are presented to identify the moment of inertia. In addition, the identification errors of the DC and PI regulator methods are also analyzed theoretically. Simulation and experimental results show that compared with the conventional identification method of the moment of inertia, the proposed DC and PI methods have improved estimation accuracy. Moreover, the presented load torque observer also has high observation precision and fast convergence speed.**

收敛

***Index Terms*—Load torque, moment of inertia, parameter identification, permanent magnet synchronous motor (PMSM), sliding mode observer (SMO).**

I. Introduction

In THE past decades, permanent magnet synchronous motor (PMSM) drives have been widely applied in various mechatronic servo systems [1]–[5]. As we know, the parameters of the drive systems, such as load torque and moment of inertia, are of great importance for improving the controller designs in industrial applications. For example, when the moment of inertia is used for designing the speed loop controller, the drive system will have higher speed tracking precision [6], [7]. In addition, when the load torque is used as the feedforward term of the reference torque, the anti load disturbance capability of the drive system will be significantly improved [8]. However, the load torque is usually unknown and the moment of inertia varies significantly with the shape and dimensions of mechanical loads. In some real PMSM drive systems, the moment of inertia and load torque are even time varying and hard to obtain online. In this case, a mismatched moment of inertia or load torque may not be powerful enough to ensure the speed control performance of the drive system. For this reason, numbers of identification algorithms of the load torque and moment of inertia have been developed.

The load torque identification methods mainly include model reference adaptive control (MRAC) [9], Kalman filter [10], [11], reduced-order observer [12], sliding mode observer (SMO) [13], [14], and so on. Because SMO has the advantages of implementation simplicity and robustness to uncertainties and disturbances, it has received more and more attention. However, most existing load torque SMO methods focus on how to depress the chattering phenomenon and neglect the influence of the parameter mismatch to the identification performance. For example, in [15]–[17], the moment of inertia values are all considered to be precise and there is no analysis to the observation performance when the moment of inertia is mismatched. Actually, a mismatched moment of inertia has great influence on the load torque observation precision especially when the drive system is under dynamic conditions.

Existing methods related to moment of inertia identification can be categorized into two major groups: offline and online identification methods. The offline identification methods mainly include calculation method, acceleration or deceleration method [18], and acceleration method with limited torque [19]. The calculation method is only applicable for known rotor structure and usually cannot calculate the combined moment of inertia of the drive system. The acceleration or deceleration method and acceleration method with limited torque have been widely used for offline moment of inertia identification, while usually with low precision, long identification time, and huge memory space. Online moment of inertia identification methods mainly include observers [20]–[22], Kalman filter [23]–[25], MRAC [26], [27], recursive least squares [28], [29], and so on. Although some of them have been applied in mechatronic servo systems successfully, there are still some problems to be solved. For example, the computational burden is large in the Kalman filter and the implementations are usually complex in most online identification algorithms mentioned above. In addition, Liu and Zhu proposed a fast determination method of moment of

计算负担

Manuscript received May 10, 2018; revised July 26, 2018; accepted September 9, 2018. Date of publication September 12, 2018; date of current version April 20, 2019. This work was supported in part by the National Key Basic Research Program of China (973 Program), under Grant 2015CB251004 and in part by the key program of National Natural Science Foundation of China under Grant 51490681. Recommended for publication by Associate Editor A. J. Marques Cardoso. *(Corresponding author: Fei Xiao.)*

The authors are with the National Key Laboratory of Science and Technology on Vessel Integrated Power System, Naval University of Engineering, Wuhan 430033, China (e-mail: wzdslcq@163.com; xfeyninger@qq.com; highershan@163.com; 66976@163.com).

Color versions of one or more of the figures in this paper are available online at http://ieeexplore.ieee.org.

Digital Object Identifier 10.1109/TPEL.2018.2870078

inertia based on the use of sinusoidal perturbation signals in [30], which can estimate the combined moment of inertia within one sinusoidal cycle of perturbation. In [31], the proposed moment of inertia algorithm is based on the time average of the product of torque reference input and motor position using periodic position reference input. However, the methods presented in [30] and [31] can be only used for offline identifications.

In this paper, a load torque observer based on sliding mode and two moment of inertia identification methods are developed for PMSM drive systems. In the load torque SMO, the mismatches of moment of inertia, electromagnetic torque, and viscous friction are all considered. Moreover, based on the property that the mismatch of the moment of inertia always causes load torque observation error under dynamic conditions, two types of moment of inertia identification methods, called direct calculation (DC) method and proportional integral (PI) regulator method, are proposed. The two methods are very applicable for offline identification of the moment of inertia and if they are used for online identification, the assumption that the load torque is constant in a short time need to be satisfied. The identification errors of the two methods are also analyzed theoretically. Simulation and experimental results demonstrate the validity of the presented scheme.

The rest of this paper is organized as follows. In Section II, the mathematical model of PMSM is introduced. In Section III, a load torque identification method and two moment of inertia identification methods are proposed. In Section IV, simulation and experimental studies are performed to demonstrate the effectiveness of the proposed moment of inertia and load torque identification algorithms. Finally, Section V draws the conclusion.

II. Mathematical Model of PMSM

In the dq-axis reference frame, the voltage equation of PMSM can be expressed as follows [32]

$$u_q = R_s i_q + (L_d i_d + \psi_f)\omega_e + L_d \frac{di_d}{dt} \tag{1a}$$

$$u_d = R_s i_d - L_q i_q \omega_e + L_q \frac{di_q}{dt} \tag{1b}$$

where $u_d, u_q, i_d, i_q, L_d, L_q, \psi_f, R_s$, and ω_e are dq-axis voltages, dq-axis currents and inductances, rotor permanent magnet flux linkage, stator resistance, and electrical angular speed, respectively.

The electromagnetic torque equation of PMSM can be described as [32] follows:

$$T_e = \frac{3}{2} P(\psi_f + (L_d - L_q) i_d) i_q \tag{2}$$

where T_e and P are electromagnetic torque and pole pair, respectively.

The mechanical equation of PMSM can be expressed as [16] follows:

$$\frac{d\omega_m}{dt} = \frac{1}{J}(T_e - T_L - F\omega_m) \tag{3}$$

where ω_m, J, T_L, and F are mechanical angular speed, moment of inertia, load torque, and viscous friction coefficient, respectively. At steady state, according to (3), T_L can be derived by

$$T_L = T_e - F\omega_m \tag{4}$$

which is independent of J. In the real PMSM drive, T_e is calculated via (2), where ψ_f, L_d, L_q can be estimated by a proper parameter identification method. In addition, F is calculated at different speeds via $F = \frac{T_e}{\omega_m}$ under no-load condition, then the approximate value of F can be derived by a curve fitting method.

III. Scheme Designs of the Load Torque and Moment of Inertia Identification

In this section, a load torque identification method based on SMO is developed with a consideration of mismatches of the moment of inertia, electromagnetic torque, and viscous friction. Based on the designed load torque observer, two types of identification methods, called DC method and PI regulator method, are proposed for the high precision identification of the moment of inertia.

A. Design of the Load Torque Observer

It is assumed that the load torque is constant within a very short time, which means $\dot{T}_L = 0$. Then, based on the mechanical equation expressed in (3), the extended state equation of PMSM can be constructed as follows:

$$\begin{cases} \dot{\omega}_m = \dfrac{1}{J}(T_e - T_L - F\omega_m) \\ \dot{T}_L = 0. \end{cases} \tag{5}$$

Taking the mechanical angular speed and load torque as the observation objects, an extended SMO can be described as follows:

$$\begin{cases} \dot{\hat{\omega}}_m = \dfrac{1}{\hat{J}}\left(\hat{T}_e - \hat{T}_L - \hat{F}\hat{\omega}_m\right) + ks_m \\ \dot{\hat{T}}_L = gs_m \end{cases} \tag{6}$$

where $\hat{T}_e, \hat{F}, \hat{\omega}_m, \hat{J}$, and $\hat{T}_L$ are the estimated values of T_e, F, ω_m, J, and T_L, respectively, k and g are the sliding mode gain and the feedback gain, respectively, $s_m = \text{sgn}(\hat{\omega}_m - \omega_m)$, and $\text{sgn}(x)$ is the sign function.

Let $e_1 = \hat{\omega}_m - \omega_m$ and $e_2 = \hat{T}_L - T_L$, then combining (5) and (6), we can get the error equation of SMO as follows:

$$\begin{cases} \dot{e}_1 = M + ks_m \\ \dot{e}_2 = gs_m \end{cases} \tag{7}$$

where

$$M = \frac{\hat{T}_e - \hat{T}_L - \hat{F}\hat{\omega}_m}{\hat{J}} - \frac{T_e - T_L - F\omega_m}{J}. \tag{8}$$

Define the sliding surface $s = e_1 = \hat{\omega}_m - \omega_m$. Based on the sliding mode control theory, it is known that the generalized sliding mode reachable condition is $s\dot{s} \le 0$. According to (7), we have

$$e_1 \dot{e}_1 = e_1(M + ks_m) \le 0. \tag{9}$$

According to (9), the sliding mode gain k satisfies

$$k \le -\|M\|. \tag{10}$$

Therefore, the parameter k can be selected as follows:

$$k = -a\|M\| \tag{11}$$

where $a \ge 1$.

When the SMO enters into the sliding mode, $e_1 = \dot{e}_1 = 0$ is satisfied. Then, (7) can be simplified as follows:

$$\begin{cases} M + ks_m = 0 \\ \dot{e}_2 = gs_m. \end{cases} \tag{12}$$

From (12), the error equation of the load torque can be derived as follows:

$$\dot{e}_2 + \frac{gM}{k} = 0. \tag{13}$$

Let $J_e = \hat{J} - J$ and substitute (8) into (13), which yields

$$\dot{e}_2 - \frac{g}{k\hat{J}}e_2 - \frac{gJ_e(T_e - T_L - F\omega_m)}{kJ\hat{J}} + \frac{g(\Delta T_e - \Delta F\omega_m)}{k\hat{J}} = 0 \tag{14}$$

where $\Delta T_e = \hat{T}_e - T_e$ and $\Delta F = \hat{F} - F$. Based on the stability theory, the stability condition of the load torque error equation expressed in (13) is given by

$$\frac{g}{k\hat{J}} < 0. \tag{15}$$

Considering $k < 0$ and $\hat{J} > 0$, we chose $g > 0$. Moreover, we can derive the analytic expression of the load torque estimation error from (14) as follows:

$$e_2 = Ce^{\frac{g}{kJ}t} - \frac{J_e(T_e - T_L - F\omega_m)}{J} + (\Delta T_e - \Delta F\omega_m) \tag{16}$$

where C is a constant. From (16), it is obvious that when $Ce^{\frac{g}{kJ}t}$ tends to zero exponentially with time t, the observation error can be expressed as follows:

$$e_2 = -\frac{J_e(T_e - T_L - F\omega_m)}{J} + (\Delta T_e - \Delta F\omega_m). \tag{17}$$

Especially, at steady state, namely, $T_e - T_L - F\omega_m = 0$, the load torque observation error is

$$e_2 = \Delta T_e - \Delta F\omega_m. \tag{18}$$

负载转矩观测器误差在动态情况下取决于 ΔTe, ΔF, Je　　稳态下取决于Je

Based on the above analysis, we can conclude that the load torque observation error is dependent of ΔT_e, ΔF, and J_e under dynamic condition. At steady state, it is independent of J_e. In Section III-C, the DC and PI regulator methods for moment of inertia identification are developed just based on this property.

B. Chattering Suppression Analysis 抖动抑制分析

As we know, the main problem of SMO is the chattering phenomenon, which degrades 降低 the identification performance of both load torque and moment of inertia. Therefore, the chattering phenomenon in the load torque observer must be suppressed for better performance. Define W as the chattering signal and when the sliding mode is reached, the error equation (7) can be rewritten as follows:

$$\begin{cases} W = M + ks_m \\ \dot{e}_2 = gs_m. \end{cases} \tag{19}$$

According to (19), the load torque error equation with chattering signal W can be derived as follows:

$$\dot{e}_2 + \frac{gM}{k} - \frac{gW}{k} = 0. \tag{20}$$

Substituting (8) into (20), yields

$$\dot{e}_2 - \frac{g}{k\hat{J}}e_2 - \frac{gJ_e(T_e - T_L - F\omega_m)}{kJ\hat{J}} + \frac{g(\Delta T_e - \Delta F\omega_m)}{k\hat{J}} - \frac{gW}{k} = 0. \tag{21}$$

Then, we can get the transfer function of (21) as follows:

$$e_2 = -\frac{\hat{J}W}{T_{sf}s + 1} + \frac{J_e(T_e - T_L - F\omega_m)}{J(T_{sf}s + 1)} - \frac{\Delta T_e - \Delta F\omega_m}{T_{sf}s + 1} \tag{22}$$

where $T_{sf} = \|k\hat{J}/g\|$. From (22), we can conclude that the chattering signal W has been suppressed by the low-pass filter with cutoff frequency 截止 $1/T_{sf}$.

Moreover, in order to further overcome the chattering problem in the presented load torque observer, the sign function $\mathrm{sgn}(\cdot)$ is replaced by a suitable saturation function as follows:

$$s_m = \mathrm{sat}(x) = \begin{cases} +1, & x > \Delta \\ x/\Delta, & \|x\| \le \Delta \\ -1, & x < -\Delta \end{cases} \tag{23}$$

where $\Delta > 0$.

Based on the above analysis, smaller $\|g/k\|$ or larger Δ will improve the chattering suppression ability of the load torque observer and at the same time, however, the dynamic performance becomes worse. Therefore, the parameters g, k, and Δ need to be selected properly in reality.

The proposed load torque observer is inspired by Zhang *et al.* [17]. In [17], only surface-mounted PMSM is considered and the mismatches of J, T_e, and F are all ignored in the designed load torque observer. However, the proposed load torque identification method in this paper not only is applicable for both surface-mounted and interior PMSMs, but also has considered the mismatches of J, T_e, and F.

本文设计的负载扭矩观测器中考虑了J，Te和F的参数不匹配。

C. Fast Identification of the Moment of Inertia

In this section, two identification algorithms of the moment of inertia are proposed, which are called DC method and PI regulator method, respectively. The DC method is applicable when the drive system has just entered into a steady state, whereas the PI regulator method is applicable when the drive system has just entered into the dynamic state from arbitrary steady state.

To derive the calculation expression of J, ΔT_e and ΔF are ignored. The influence of ΔT_e and ΔF on the estimation error of J will be analyzed in the next section. In this case, (17) can

be rewritten as

$$e_2 = -\frac{J_e(T_e - T_L - F\omega_m)}{J}. \tag{24}$$

Notice that there are only two unknown variables T_L and J in (24); thus, if the load torque T_L has been known, the moment of inertia J can be calculated directly if the drive system is at dynamic state. The load torque can be obtained via (4) at steady state directly. Moreover, as mentioned above, the load torque identification error is independent of the estimation error of the moment of inertia at steady state. Therefore, we can also identify the load torque using the proposed SMO with an arbitrary initial moment of inertia at steady state.

1) DC Method: When the drive system has entered into the steady state at time step k, the load torque T_L can be calculated by

$$T_L(k) = T_e(k) - F\omega_m(k). \tag{25}$$

It is assumed that $T_L(k)$ is constant from time step k_1 to k and the exponential term in (16) has tended to zero at time step k_1. Then, according to (24), the moment of inertia can be calculated directly by the following expression:

$$\hat{J}(k) = \frac{T_e(k_1) - T_L(k) - F\omega_m(k_1)}{T_e(k_1) - \hat{T}_L(k_1) - F\omega_m(k_1)}\hat{J}_{\text{init}} \tag{26}$$

where $\hat{J}(k)$ is the calculation value of the moment of inertia at time step k and $\hat{J}_{\text{init}}$ is the initial moment of inertia value, which is used for estimating the load torque $\hat{T}_L(k_1)$. Let $\Delta k = k - k_1$ and if Δk is too large, the assumption that the load torque is constant in the past time steps Δk is hard to be satisfied. If Δk is too small, there may be a larger calculation error because of the sampling noise or other nonideal factors.

2) PI Regulator Method: As mentioned above, the load torque observation error always exists at dynamic state when $J_e \neq 0$. Rewrite (24) as the discrete time form, which yields

$$J_e(k) = \frac{J}{T_L(k) + F\omega_m(k) - T_e(k)}e_2(k) \tag{27}$$

where k is the time step. Therefore, a PI regulator can be employed to identify the moment of inertia and the update rule is given as follows:

$$\begin{aligned}\hat{J}(k+1) = \hat{J}(k) + s_T(k)\left(k_p e_2(k) + T_s k_i e_2(k)\right) \\ - s_T(k-1)k_p e_2(k-1)\end{aligned} \tag{28}$$

where k_p and k_i are proportional and integral gains, respectively, T_s is the sampling time, and

$$s_T(k) = \text{sgn}\left(T_e(k) - T_L(k) - F\omega_m(k)\right). \tag{29}$$

The reason for replacing $J/(T_e(k) - T_L(k) - F\omega_m(k))$ with $s_T(k)$ is that when the drive system tends to arbitrary steady state, the $J/(T_e(k) - T_L(k) - F\omega_m(k))$ term will tend to infinity, which may cause identification failure.

In addition, taking into account that the two moment of inertia identification algorithms are valid only when the load torque is constant in a short time, better offline estimation precision can be expected because the mentioned assumption can be satisfied easily in this case. When they are used for online identification, the identification performance is closely related to the load characteristics.

D. Identification Error Analysis of the Moment of Inertia

In this section, the influence of mismatches of electromagnetic torque T_e and viscous friction coefficient F on the identification error of moment of inertia will be analyzed.

1) Identification Error Analysis of the DC Method: Let $\hat{\hat{T}}_L(k_1)$ be the approximate value of $\hat{T}_L(k_1)$ with considering the estimation errors of T_e and F. According to (17) and (24), we have

$$\hat{\hat{T}}_L(k_1) = \hat{T}_L(k_1) + (\Delta T_e(k_1) - \Delta F\omega_m(k_1)). \tag{30}$$

According to (26), the moment of inertia is calculated by the following expression in real PMSM drives:

$$\hat{J}(k) = \frac{\hat{T}_e(k_1) - \hat{T}_L(k) - \hat{F}\omega_m(k_1)}{\hat{T}_e(k_1) - \hat{\hat{T}}_L(k_1) - \hat{F}\omega_m(k_1)}\hat{J}_{\text{init}}. \tag{31}$$

Substituting (18) and (30) into (31), we can derive

$$\begin{aligned}\hat{J}(k) = &\frac{T_e(k_1) - T_L(k) - F\omega_m(k_1)}{T_e(k_1) - \hat{T}_L(k_1) - F\omega_m(k_1)}\hat{J}_{\text{init}} \\ &+ \frac{\Delta T_e(k_1) - \Delta T_e(k) + \Delta F(\omega_m(k) - \omega_m(k_1))}{T_e(k_1) - \hat{T}_L(k_1) - F\omega_m(k_1)}\hat{J}_{\text{init}}.\end{aligned} \tag{32}$$

Combining (26) and (32), the calculation error of J is

$$J_{e\text{DC}} = \frac{\Delta T_e(k_1) - \Delta T_e(k) + \Delta F(\omega_m(k) - \omega_m(k_1))}{T_e(k_1) - \hat{T}_L(k_1) - F\omega_m(k_1)}\hat{J}_{\text{init}}. \tag{33}$$

From (33), we can see that $J_{e\text{DC}}$ is dependent of $\hat{J}_{\text{init}}$, ΔT_e, and ΔF. On one hand, ΔT_e and ΔF can be effectively reduced by some proper parameter estimation methods, as mentioned in Section II. On the other hand, compared with ΔT_e and ΔF, $\hat{J}_{\text{init}}$ has a more direct impact on $J_{e\text{DC}}$. In real PMSM drives, small $\hat{J}_{\text{init}}$ is usually selected to decrease the calculation error of J.

2) Identification Error Analysis of the PI Regulator Method: The PI regulator method aims to minimize $\|e_2\| = \|\hat{T}_L(k_2) - T_L(k)\|$ and once $\|e_2\| \to 0$, the exact J will be obtained. However, in real PMSM drives, we have to use $\|\hat{e}_2\| = \|\hat{T}_L(k_2) - \hat{T}_L(k)\|$ instead of $\|e_2\|$ when mismatches of T_e and F are considered, where

$$\hat{T}_L(k) = T_L(k) + \Delta T_e(k) - \Delta F\omega_m(k). \tag{34}$$

Combining (17) and (34), we have

$$\begin{aligned}\hat{T}_L(k_2) - \hat{T}_L(k) = &-\frac{J_e(T_e(k_2) - T_L(k) - F\omega_m(k_2))}{J} \\ &+ (\Delta T_e(k_2) - \Delta F\omega_m(k_2)) - (\Delta T_e(k) - \Delta F\omega_m(k)).\end{aligned} \tag{35}$$

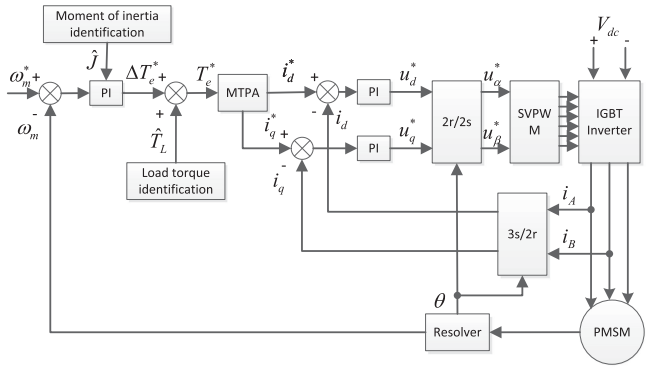

Fig. 1. Block diagram of the PMSM drive system.

When the PI regulator method is convergence, which means $\hat{T}_L(k_2) - \hat{T}_L(k) = 0$, we can derive

$$J_{e\mathrm{PI}} = \frac{\Delta T_e(k_2) - \Delta T_e(k) + \Delta F(\omega_m(k) - \omega_m(k_2))}{T_e(k_2) - T_L(k) - F\omega_m(k_2)} J. \tag{36}$$

In the PI regulator method, it usually costs short time to reach the convergence state and $\omega_m(k)$ and $\omega_m(k_2)$ are usually closed to each other. Therefore, we can conclude that ΔF has limited influence on $J_{e\mathrm{PI}}$ from (36). Besides, considering $F, \Delta F$ are usually small, let $\Delta F\omega_m(k_2) \approx \Delta F\omega_m(k)$ and $F\omega_m(k_2) \approx F\omega_m(k)$ to simplify analysis. Then, according to (36), yields

$$J_{e\mathrm{PI}} \approx \frac{\Delta T_e(k_2) - \Delta T_e(k)}{T_e(k_2) - T_e(k)} J. \tag{37}$$

Let $\Delta T_e(k_2) = mT_e(k_2), \Delta T_e(k) = nT_e(k)$, then (37) is rewritten as

$$J_{e\mathrm{PI}} \approx \left(m + \frac{m-n}{\frac{T_e(k_2)}{T_e(k)} - 1} \right) J. \tag{38}$$

It is obvious that the estimation error of electromagnetic torque has direct influence on $J_{e\mathrm{PI}}$. To decrease the identification error of moment of inertia, the estimation precision and consistency of electromagnetic torque should be guaranteed, which means smaller m, n and $\|m - n\|$.

IV. Simulation and Experimental Studies

In this section, the simulation and experimental studies are performed to demonstrate the effectiveness of the proposed moment of inertia and load torque identification algorithms. The block diagram of the PMSM drive system is given in Fig. 1. The identified value of moment of inertia is used to tuning the proportion coefficient of speed controller online, which guarantees favorable speed control performance. In this paper, the method in [33] is employed to design the PI regulators of speed and current loops. The identified load torque is used as the feedforward of the reference torque, which improves the ability to resist the load disturbance. The design parameters and specification of PMSM are listed in Table I.

TABLE I
Design Parameters and Specification of PMSM

Parameters	Value
Rated speed	3000 rpm
Rated torque	955 Nm
Rated power	300 kW
Rated current	500 A
Number of pole pairs	3
Nominal stator resistance	0.0041 Ω
Nominal rotor PM flux linkage	0.29 Wb
Nominal d-axis inductance	0.28 mH
Nominal q-axis inductance	0.61 mH
Nominal moment of inertia of rotor	1.39 kg·m^2
Nominal viscous friction coefficient	0.19
DC link voltage	900 V

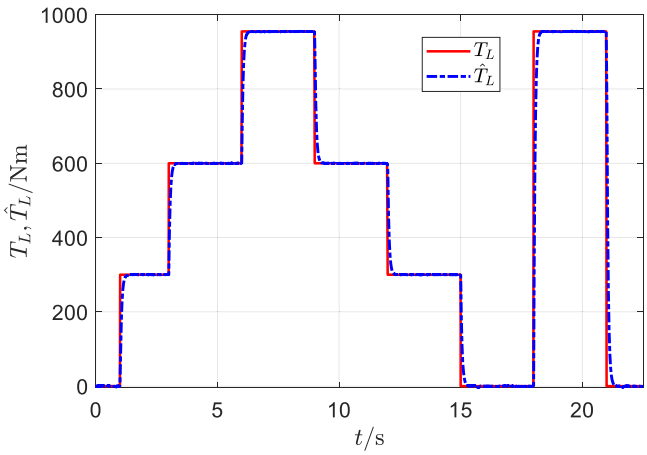

Fig. 2. Load torque identification curves under different load torque in the simulation.

A. Simulation Study

First, the load torque identification is performed. In the simulation and experimental studies, the observation parameters are selected to be $\Delta = 0.5$, $k = -1500$, and $g = 80\,000$ for the best identification performance.

The load torque identification curves under different load torque are shown in Fig. 2. We can see that the estimated values can always follow the step-change load torque and without any overshooting. Fast load torque identification is beneficial to improve the antidisturbance capacity of the drive system.

Set the load torque, reference speed, and initial moment of inertia to be 300 N·m, 1000 r/min, and 0.973 kg·m^2, respectively; then, Fig. 3 shows the torque and speed curves when using the DC method to estimate the moment of inertia. It is assumed that T_e can always track T_e^* well and therefore, we use T_e^* instead of T_e for reducing the calculation error. If the rotor speed reaches the given value and in the following 10 ms the maximum speed error is less than 1 r/min, then the drive system can be considered to have reached steady state. As shown in Fig. 3, the system reaches steady state at time 1.02 s and the identified value of the load torque is 302.9 N·m, which can be regarded as

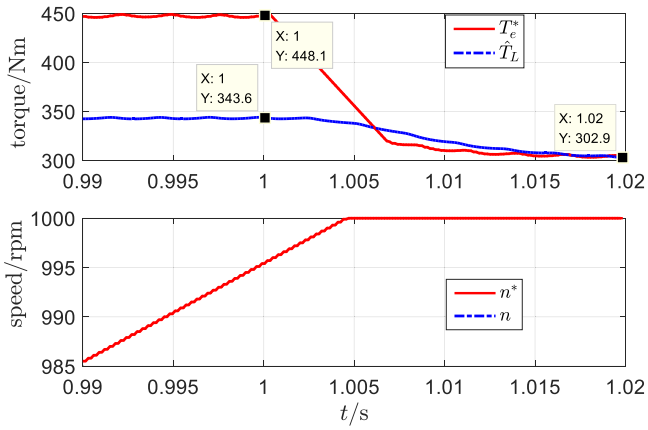

Fig. 3. Torque and speed curves using the DC method in the simulation.

TABLE II
PERFORMANCE OF THE DC METHOD WITH DIFFERENT Δt

Parameters	Values					
Δt(ms)	15	20	25	30	35	40
J_c(kg·m^2)	1.84	1.36	1.36	1.37	1.38	1.37
Error(%)	32.4	2.2	2.2	1.4	0.7	1.4

TABLE III
PERFORMANCE OF THE PI REGULATOR METHOD WITH DIFFERENT k_p, k_i

Parameters	k_p	k_i	t_s(ms)	σ(%)	e_{ss}(kg·m^2)
Values	0.002	0.2	70.0	0	0
	0.002	0.8	27.8	10.1	0
	0.002	1.5	32.3	21.9	0
	0.008	0.2	171.1	0	0
	0.008	0.8	13.1	0	0
	0.008	1.5	13.5	3.3	0
	0.020	0.2	269.1	2.4	0
	0.020	0.8	31.6	4.0	0
	0.020	1.5	15.2	5.7	0

the real load torque for the calculation of the moment of inertia. Let $\Delta t = T_s \Delta k$ and when $\Delta t = 20$ ms, from Fig. 3, we have $T_e = 448.1$ N·m, $\hat{T}_L = 343.6$ N·m, and $n = 995.4$ r/min. Then, according to (26), the calculated value of J is 1.36 kg·m^2, which is very close to the nominal value of 1.39 kg·m^2.

Table II lists the calculation results of the moment of inertia with different Δt. It is shown that when $\Delta t = 15$ ms, the calculation error is 32.4%, whereas when $\Delta t \geq 20$ ms, the maximum estimation error is 2.2%.

Table III lists the estimated values of the moment of inertia based on the PI regulator method with different k_p and k_i, where the initial $\hat{J}_0$ is selected as 0.5 times of the nominal value. In Table III, t_s is the regulating time (the error band is $\pm 2\%$ of the steady-state value), σ is the overshooting value, and e_{ss} is the steady-state error. We can see that when $k_p = 0.008$ and $k_i = 0.8$, it has the best identification performance with $t_s = 13.1$ ms, $\sigma = 0$, and $e_{ss} = 0$. In the following, the selected k_p and k_i parameters will be always used if there is no special description.

TABLE IV
REGULATING TIMES OF THE MOMENT OF INERTIA IDENTIFICATION ALGORITHM BASED ON THE PI REGULATOR METHOD WITH DIFFERENT k_0

Parameters	Values					
k_0	0.5	0.7	0.9	1.2	1.4	1.6
t_s(ms)	13.1	8.5	4.7	6.3	10.7	15.8

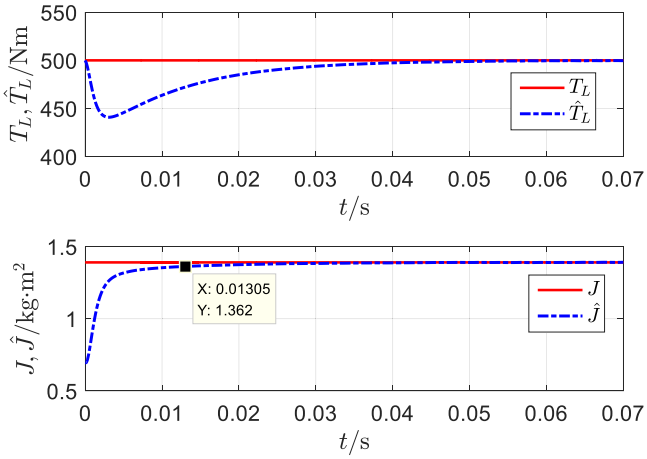

Fig. 4. Load torque and moment of inertia identification curves based on SMO and the PI regulator method in the simulation.

Let $\hat{J}_0$ be k_0 times of the nominal value, then the regulating times of the moment of inertia identification algorithm based on the PI regulator method with different k_0 are listed in Table IV. It is shown that the regulating time t_s is proportional to $\|k_0 - 1\|$. The overshooting value and steady-state error not listed in Table IV are both zeros in all cases. Fig. 4 shows the load torque and moment of inertia identification curves based on SMO and the PI regulator method. We can see that the identification error of the moment of inertia converges to zero fast without any overshooting and oscillation.

Based on the simulation results, we can conclude that the PI regulator method has higher identification precision and faster convergence speed than the DC method, which is the reason why the PI regulator method is utilized when the drive system enters into dynamic state from steady state.

B. Experimental Study

In order to further verify the effectiveness of the proposed scheme, an experimental study is performed based on the experiment platform shown in Fig. 5. In the experiment, the conventional acceleration or deceleration method and the proposed DC and PI regulator methods are all employed to evaluate the identification performance. In the conventional acceleration or deceleration method, the influence of $F\omega_m$ is ignored. Keep electromagnetic torque T_e and load torque T_L constant within time ΔT, then the estimated moment of inertia $\hat{J}_{\text{conv}}$ can be derived by

$$\hat{J}_{\text{conv}} = \frac{\Delta T}{\Delta \omega_m}(T_e - T_L) \tag{39}$$

where $\Delta \omega_m = \omega_m(t + \Delta T) - \omega_m(t)$.

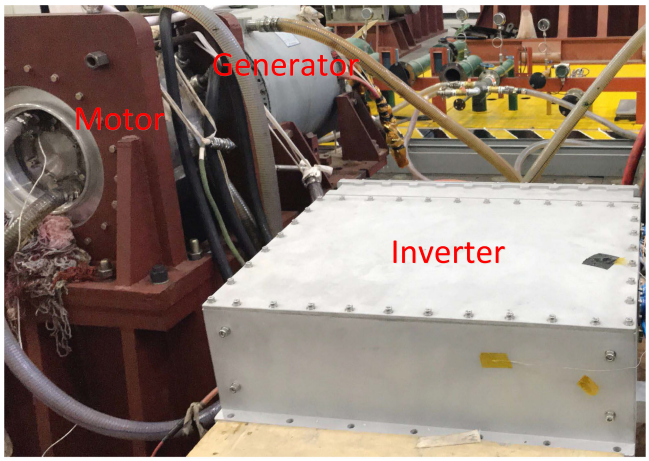

Fig. 5. Experiment platform.

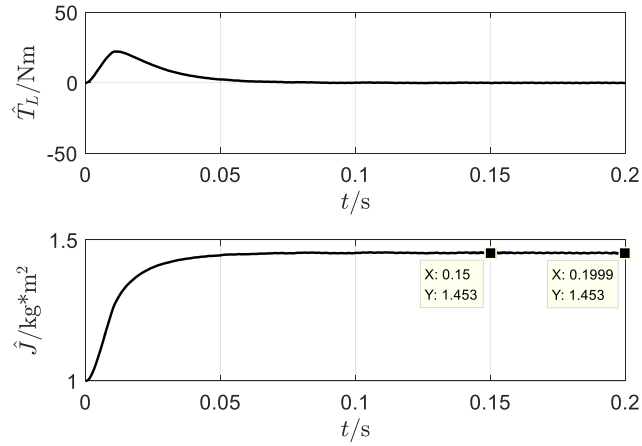

Fig. 6. Load torque and moment of inertia estimation curves of the motor based on the PI regulator method.

TABLE V
MOMENT OF INERTIA ESTIMATED VALUES OF THE MOTOR USING THE CONVENTIONAL ACCELERATION OR DECELERATION METHOD

Parameters	Values			
T_e(N·m)	-300	-150	150	300
$\Delta\omega_m$(rad/s)	-300	-300	300	300
ΔT(s)	1.461	2.952	3.040	1.505
$\hat{J}_{conv}$(kg·m^2)	1.461	1.476	1.528	1.505
Error(%)	5.1	6.2	9.9	8.3
$\bar{J}_{conv}$(kg·m^2)	1.493			

TABLE VI
MOMENT OF INERTIA ESTIMATED VALUES OF THE MOTOR USING THE DC METHOD

Parameters	Values				
Δt(ms)	20	25	30	35	40
$\hat{J}_{DC}$(kg·m^2)	1.451	1.423	1.446	1.427	1.439
Error(%)	4.4	2.4	4.0	2.7	3.5
$\bar{J}_{DC}$(kg·m^2)	1.437				

First, uncouple the motor and generator and the moment of inertia estimated values of the motor using the conventional acceleration or deceleration method with different electromagnetic torques are listed in Table V, in which $\Delta\omega_m$ is set to be -300 or 300 rad/s. It is shown that the average moment of inertia $\bar{J}_{\text{conv}}$ is 1.493 kg·m^2, which is 7.4% larger than the nominal value.

The moment of inertia estimated values of the motor based on the proposed DC method are listed in Table VI. It is demonstrated that the identified values are very close to each other with different Δt. The average value $\bar{J}_{\text{DC}}$ is 1.437 kg·m^2, which is 3.4% larger than the nominal value.

Keep the drive system at 500 r/min speed under unload condition and select the initial $\hat{J}_0$ as 1 kg·m^2, then set the reference speed to be 1000 r/min and the drive system will enter into the dynamic state. Fig. 6 exhibits the estimated values of the load torque and moment of inertia using the PI regulator method. It is shown that the estimated value of the moment of inertia converges fast and the convergence value is 1.453 kg·m^2, which is 4.5% larger than the nominal value.

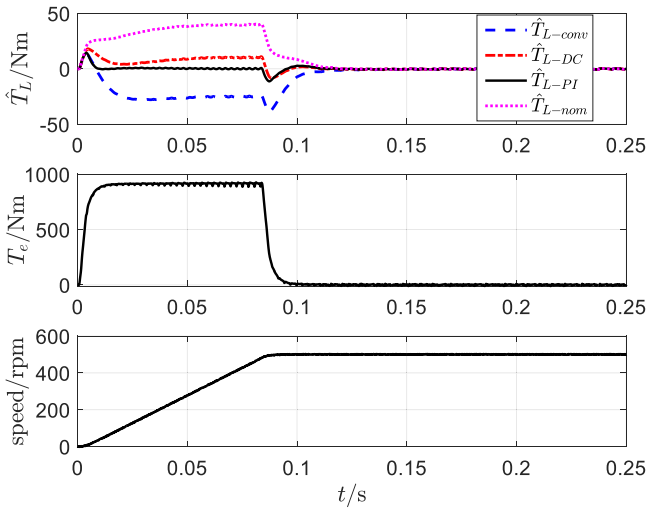

Fig. 7. Curves of load torque, electromagnetic torque, and speed using different estimated values of J.

In order to verify the precision of the three moment of inertia identification methods, we use $\hat{J}_{\text{conv}}$, $\hat{J}_{\text{DC}}$, $\hat{J}_{\text{PI}}$, and nominal value J_{nom} to identify the load torque under unload condition, respectively. The curves of the load torque, electromagnetic torque, and speed using different estimated values of J are exhibited in Fig. 7. It is demonstrated that under the dynamic condition, the load torque has the largest identification error when using the nominal moment of inertia, which means the nominal moment of inertia is not accurate enough. When using the PI regulator method to obtain the moment of inertia for online load torque identification, the identification error is the smallest, which implies the PI regulator method has the highest identification precision of the moment of inertia according to the analysis mentioned above. Additionally, compared with the proposed two methods, the identification accuracy of the conventional acceleration or deceleration method is lower.

Couple the driving motor, the torque meter, and permanent synchronous generator with no load, then the identified values

TABLE VII
IDENTIFIED VALUES OF THE COMBINED MOMENT OF INERTIA USING THE THREE METHODS

methods	$\hat{J}$(kg·m^2)
conventional method	2.861
direct calculation method	2.752
PI regulator mehtod	2.705

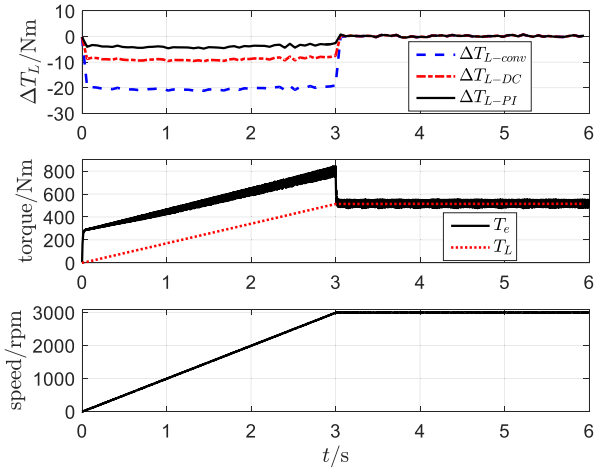

Fig. 8. Curves of torque and speed with different estimated values of the combined moment of inertia.

of the overall combined moment of inertia using the three methods are listed in Table VII. Connect the resistance load to the generator, then there is an approximate linear relationship between the load torque T_L and the mechanical angular velocity ω_m as follows:

$$T_L = D\omega_m \tag{40}$$

where D is determined by the resistance load. Keep the resistance load constant and record the load torque T_L from the torque meter at different ω_m, then the parameter D can be calculated by the least square method.

Fig. 8 exhibits the curves of torque and speed with different estimated values of the combined moment of inertia, where $\Delta T_L = \hat{T}_L - T_L$ and T_L is calculated by (40). It is illustrated that under the dynamic condition, the load torque identification error is the smallest when using the PI regulator method to obtain the moment of inertia for online load torque identification, which indicates the PI regulator method has the highest moment of inertia identification precision. Compared with the PI regulator and DC methods, the conventional acceleration or deceleration method has lower estimation accuracy.

Fig. 9 shows the curves of the current, torque, and speed with sudden load change. First, keep the speed at 3000 r/min and through the load torque observer, we can obtain the information that the torque load is about 510 N·m. Dump all resistance load suddenly and we can see that the speed fluctuations with torque feedforward compensation and without torque feedforward compensation are about 26 and 62 r/min, respectively. When the resistance load is added suddenly, it is shown that the load torque estimated value is about 900 N·m, which is close

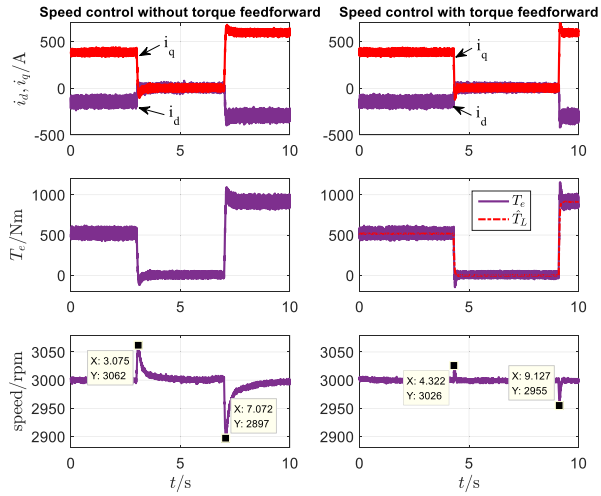

Fig. 9. Curves of the current, torque, and speed with sudden load change.

to the rated torque. Moreover, we can also see that when using the load torque estimated value as the torque feedforward compensation, the speed fluctuation is smaller. The experimental results demonstrate the validity of the proposed load torque and moment of inertia identification methods.

V. CONCLUSION

Existing load torque observers based on sliding mode usually ignore the influence of mismatches of moment of inertia, electromagnetic torque, and viscous friction on the observation performance. In this paper, a novel load torque SMO is designed and utilizing the observation error caused by the mismatch of the moment of inertia, two methods called DC calculation and PI regulator are developed to estimate the moment of inertia. The identification errors of the two methods are also analyzed theoretically. Simulation and experimental results show that the proposed DC and PI methods have improved estimation precision and faster convergence speed compared with the conventional moment of inertia identification method. Moreover, the presented load torque SMO also has high estimation precision and fast convergence speed. It is also demonstrated that when the estimated load torque is used as the feedforward term of the reference torque, the drive system has improved antidisturbance capability.

REFERENCES

[1] A. Khlaief, M. Bendjedia, M. Boussak, and M. Gossa, "A nonlinear observer for high-performance sensorless speed control of IPMSM drive," *IEEE Trans. Power Electron.*, vol. 27, no. 6, pp. 3028–3040, Jun. 2012.
[2] T. Miyajima, H. Fujimoto, and M. Fujitsuna, "A precise model-based design of voltage phase controller for IPMSM," *IEEE Trans. Power Electron.*, vol. 28, no. 12, pp. 5655–5664, Dec. 2013.
[3] X. G. Zhang, L. Z. Sun, K. Zhao, and L. Sun, "Nonlinear speed control for PMSM system using sliding-mode control and disturbance compensation techniques," *IEEE Trans. Power Electron.*, vol. 28, no. 3, pp. 1358–1365, Mar. 2013.
[4] H. Nakai, H. Ohtani, E. Satoh, and Y. Inaguma, "Development and testing of the torque control for the permanent-magnet synchronous motor," *IEEE Trans. Ind. Electron.*, vol. 52, no. 3, pp. 800–806, Jun. 2005.
[5] K. H. Kim and M. J. Youn, "A nonlinear speed control for a PM synchronous motor using a simple disturbance estimation technique," *IEEE Trans. Ind. Electron.*, vol. 49, no. 3, pp. 524–535, Jun. 2002.

[6] S. Li and Z. Liu, "Adaptive speed control for permanent-magnet synchronous motor system with variations of load inertia," *IEEE Trans. Ind. Electron.*, vol. 56, no. 8, pp. 3050–3059, Aug. 2009.
[7] G. Zhang, "Speed control of two-inertia system by PI/PID control," *IEEE Trans. Ind. Electron.*, vol. 47, no. 3, pp. 603–609, Jun. 2000.
[8] Y. Zhang, C. M. Akujuobi, W. H. Ali, C. L. Tolliver, and L.-S. Shieh, "Load disturbance resistance speed controller design for PMSM," *IEEE Trans. Ind. Electron.*, vol. 53, no. 4, pp. 1198–1208, Jun. 2006.
[9] D. G. Xu and G. Yang, "An approach to torque ripple compensation for high performance PMSM servo system," in *Proc. IEEE 35th Annu. Power Electron. Spec. Conf.*, 2004, pp. 3256–3259.
[10] H. Wang, Y. K. Wang, and X. B. Wang, "Speed and load torque estimation of SPMSM based on Kalman filter," in *Proc. IEEE Int. Conf. Mechatronics Automat.*, Beijing, China, Aug. 2015, pp. 808–813.
[11] K. Kyslan, V. Šlapák, V. Fedák, F. Ďurovský, and K. Horváth, "Design of load torque and mechanical speed estimator of PMSM with unscented Kalman filter—An engineering guide," in *Proc. 19th Int. Conf. Elect. Drives Power Electron.*, Dubrovnik, Croatia, Oct. 2017, pp. 297–302.
[12] H. Y. Zhang, H. P. Xu, C. Fang, and C. Xiong, "Design of a novel speed controller for direct-drive permanent magnet synchronous motor based on reduced-order load torque observer," in *Proc. IEEE Transp. Electrific. Conf. Expo, Asia–Pac.*, 2017, pp. 1–6.
[13] H. Kim, J. Son, and J. Lee, "A high-speed sliding-mode observer for the sensorless speed control of a PMSM," *IEEE Trans. Ind. Electron.*, vol. 58, no. 9, pp. 4069–4077, Sep. 2011.
[14] Z. Y. Tang, P. Pei, M. Wen, and Z. Q. Shi, "Two novel reaching laws and their use in sliding mode control of EHA," in *Proc. IEEE Int. Conf. Inf. Automat.*, Aug. 2015, pp. 1441–1446.
[15] C. F. Zhang, L. Jia, and J. He, "Load torque observer based sliding mode control method for permanent magnet synchronous motor," in *Proc. 25th Chin. Control Decis. Conf.*, 2013, pp. 550–555.
[16] X. G. Zhang and B. S. Hou, "Novel reaching law-based sliding-mode load torque observer for PMSM," in *Proc. 19th Int. Conf. Elect. Mach. Syst.*, 2016, pp. 1–5.
[17] X. G. Zhang, L. Sun, and K. Zhao, "Sliding mode control of PMSM based on a novel load torque sliding mode observer," *Proc. CSEE*, vol. 32, no. 3, pp. 111–116, Jan. 2012.
[18] X. W. Wang, "Inertia identification of permanent magnetic ac servo system," *Mach. Tool Hydraul.*, vol. 36, no. 8, pp. 299–300, Aug. 2008.
[19] B. Zhang, Y. H. Li, and Y. S. Zuo, "A DSP-based fully digital PMSM servo drive using on-line self-tuning PI controller," in *Proc. 3rd Int. Power Electron. Motion Control Conf.*, 2000, vol. 2, pp. 1012–1017.
[20] S. M. Yang and Y. J. Deng, "Observer-based inertia identification for auto-tuning servo motor drivers," in *Proc. Ind. Appl. Conf.*, 2005, vol. 2, pp. 968–972.
[21] Y. Gao, M. Yang, Y. Yu, and D. G. Xu, "Disturbance observer based low speed control of PMSM servo system," *Proc. CSEE*, vol. 25, no. 22, pp. 125–129, Nov. 2005.
[22] N. Kim, H. Moon, and D. Hyun, "Inertia identification for the speed observer of the low speed control of induction machines," *IEEE Trans. Ind. Appl.*, vol. 32, no. 6, pp. 1371–1379, Nov./Dec. 1996.
[23] C. M. De, E. G. Caratti, and H. A. Grundling, "Design of a position servo with induction motor using self-tuning regulator and Kalman filter," in *Proc. Conf. Rec. IAS Annu. Meeting*, 2000, vol. 3, pp. 1613–1618.
[24] S. Bolognani, L. Tubiana, and Z. Mauro, "Extended Kalman filter tuning in sensorless PMSM drives," *IEEE Trans. Ind. Electron.*, vol. 39, no. 6, pp. 1741–1747, Nov./Dec. 2003.
[25] S. Hong, H. Kim, and S. Sul, "A novel inertia identification method for speed control of electric machine," in *Proc. IEEE 22nd Int. Conf. Ind. Electron., Control, Instrum.*, Taipei, Taiwan, R.O.C., Aug. 1996, vol. 2, pp. 1234–1239.
[26] L. A. Gu, L. J. Liu, and X. F. Liu, "Researches on the key technologies of online identification of inertia of PMSM," *Mach. Des. Manuf.*, vol. 4, pp. 29–32, Apr. 2017.
[27] Y. Guo, L. Huang, Y. Qiu, and M. Muramatsu, "Inertia identification and auto-tuning of induction motor using MRAS," in *Proc. 3rd Int. Conf. Power Electron. Motion Control*, Beijing, China, Aug. 2000, vol. 2, pp. 1006–1011.
[28] K. Y. Wang, J. Chiasson, M. Bodson, and L. M. Tolbert, "A nonlinear least-squares approach for identification of the induction motor parameters," *IEEE Trans. Autom. Control*, vol. 50, no. 10, pp. 1622–1628, Oct. 2005.
[29] F. J. Lin, "Robust speed-controlled induction-motor drive using EKF and RLS estimators," *Inst. Elect. Eng. Proc.—Elect. Power Appl.*, vol. 143, no. 3, pp. 186–192, May 1996.
[30] K. Liu and Z. Q. Zhu, "Fast determination of moment of inertia of permanent magnet synchronous machine drives for design of speed loop regulator," *IEEE Trans. Control Syst. Technol.*, vol. 25, no. 5, pp. 1816–1824, Sep. 2017.
[31] F. Andoh, "Moment of inertia identification using the time average of the product of torque reference input and motor position," *IEEE Trans. Power Electron.*, vol. 22, no. 6, pp. 2534–2542, Nov. 2007.
[32] Y. Miao, H. Ge, M. Preindl, J. Ye, B. Cheng, and A. Emadi, "MTPA fitting and torque estimation technique based on a new flux-linkage model for interior-permanent-magnet synchronous machines," *IEEE Trans. Ind. Appl.*, vol. 53, no. 6, pp. 5451–5460, Nov./Dec. 2017.
[33] K. Liu and Z. Q. Zhu, "Parameter estimation of PMSM for aiding PI regulator design of field oriented control," in *Proc. Int. Conf. Elect. Mach. Syst.*, Oct. 2014, pp. 2705–2711.

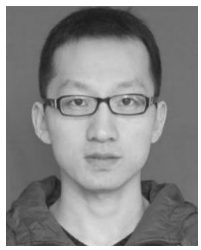

Chuanqiang Lian received the B.S. degree in automation from Tsinghua University, Beijing, China, in 2008, and the M.S. and Ph.D. degrees from the College of Mechatronic Engineering and Automation, National University of Defense Technology, Changsha, China, in 2010 and 2016, respectively.

He is currently a Lecturer with the National Key Laboratory of Science and Technology on Vessel Integrated Power System, Naval University of Engineering, Wuhan, China. He has coauthored more than ten papers in international journals and conferences. His research interests include ac motor control, machine learning, and autonomous vehicles.

Fei Xiao was born in Hubei Province, China, in 1977. He received the B.S. and M.S. degrees from Naval University of Engineering, Wuhan, China, in 1999 and 2001, respectively, and the Ph.D. degree from Zhejiang University, Hangzhou, China, in 2012, all in electrical engineering.

From 2003 to 2009, he was a Lecturer with Naval University of Engineering, where he was promoted to an Associate Professor in 2009 and to a Full Professor in 2012. He is currently the Committee Member of the Department of Energy and Transportation in China Ministry of Science and Technology. His research interests include renewable energy generation, modeling and control of power electronics system, and high-voltage large-capacity power electronics equipment.

Shan Gao received the B.S. and Ph.D. degrees in electrical engineering from the Huazhong University of Science and Technology, Wuhan, China, in 2008 and 2016, respectively.

He is currently with the National Key Laboratory of Science and Technology on Vessel Integrated Power System, Naval University of Engineering, Wuhan, China. His research interests include large-power multilevel inverters, and electric vehicle drives.

Jilong Liu was born in Hebei Province, China, in 1988. He received the B.S. and Ph.D. degrees from the School of Electrical Engineering, Xi'an Jiaotong University, Xi'an, China, in 2010 and 2015, respectively.

He is currently an Associate Professor with Naval University of Engineering, Wuhan, China. His research interests include modular multilevel converters and position-sensorless control of permanent magnet synchronous motors.